Synthesis and Characterization of Novel Substituted 3,6-Di(2-pyridyl)pyridazine Metal-Coordinating Ligands

Richard Hoogenboom,[a] Guido Kickelbick,[b] and Ulrich S. Schubert*[a]

Keywords: Cycloadditions / Heterocycles / Metal-coordination / 2D NMR spectroscopy

The synthesis of novel functionalized 3,6-di(2-pyridyl)pyridazines via an inverse electron demand Diels–Alder reaction between the corresponding 3,6-di(2-pyridyl)-1,2,4,5-tetrazine and various alkynes is reported. The resulting 3,6-di(2-pyridyl)pyridazines were investigated using X-ray crystallography, IR spectroscopy, and NMR spectroscopy, whereby several 2D NMR spectroscopic techniques were exploited to conclusively assign all proton- and carbon-resonances. In addition, it was demonstrated that the functionalized 3,6-di(2-pyridyl)pyridazines are capable of forming [2 × 2] grid-like metal complexes with copper(I) and silver(I) ions.

Introduction

Metal-complexing ligands have attracted much attention in the last few decades, when they have been used in the construction of large, well-defined supramolecular architectures with many interesting properties, such as reversible binding behavior, and special optical, magnetic and electrochemical features.[1] 3,6-Di(2-pyridyl)pyridazines represent one of the most interesting ligand-systems in this area. These compounds can act as metal-coordinating ligands for copper(I),[2] silver(I),[3,4] and nickel(II)[5] ions, resulting in grid-like metal complexes (Figure 1). Moreover, many binuclear complexes of these ligands with, for example, nickel(II),[6] copper(II),[7] and platinum(II)[8] ions have been reported. The introduction of functional groups would allow the incorporation of the ligands and the corresponding metal complexes into larger assemblies and polymers. In the latter case, the ligands could, for example, be utilized as initiators.[9] Highly functionalized pyridazines are easily accessible via an inverse electron demand Diels−Alder reaction between 1,2,4,5-tetrazines and a wide range of acetylenes, whereby the 1,2,4,5-tetrazine acts as the electron-deficient diene.[10] Reactions of this type have been reported with many different substituents on the 3- and 6-positions of the 1,2,4,5-tetrazines.[11−17] Members of this heterocyclic class of compounds have attracted much attention[10] in the field of organic chemistry, both in mechanistic investigations[11,13,16,17] and natural product synthesis.[14,15,17]

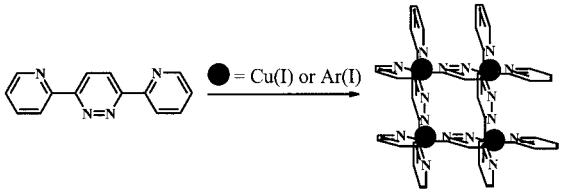

Figure 1. Self-assembly of 3,6-di(2-pyridyl)pyridazine into a grid-like metal complex with copper(I) or silver(I) ions

Although many substituted 3,6-di(2-pyridyl)pyridazines have been synthesized, the direct synthesis of hydroxy-functionalized ligands has not been reported yet. In addition, metal complexation with copper(I) and silver(I) ions to form grid-like structures has, up to now, only been described for unsubstituted and 6,6′′-substituted 3,6-di(2-pyridyl)pyridazines. Herein, we report our investigations concerning inverse-type Diels−Alder reactions of 3,6-di(2-pyridyl)tetrazine with functionalized acetylenes, the characterization of the resulting 4,5-disubstituted 3,6-di(2-pyridyl)pyridazines, and the metal complexation of these ligands to form grid-like complexes with copper(I) and silver(I) ions.

Results and Discussion

Synthesis of Substituted 3,6-Di(2-pyridyl)pyridazines

4,5-Disubstituted pyridazines can be synthesized by an inverse electron demand Diels−Alder reaction of the corresponding 1,2,4,5-tetrazines with alkenes or alkynes; after the reaction with alkenes, the 1,4-dihydropyridazines are obtained, which undergo (spontaneous) oxidation to give

[a] Laboratory of Macromolecular Chemistry and Nanoscience, Eindhoven University of Technology and Dutch Polymer Institute (DPI),
P. O. Box 513, 5600 MB Eindhoven, The Netherlands
Fax: (internat.) + 31-40-247-4186
E-mail: u.s.schubert@tue.nl
[b] Institute of Materials Chemistry, Vienna University of Technology,
Getreidemarkt 9, 1060 Wien, Austria

the pyridazines.[10,12,16] The synthesis of 3,6-di(2-pyridyl)tetrazine, and its utilization in inverse-type Diels−Alder reactions, was first described by Butte and Case.[12] By coupling two 2-cyanopyridines with hydrazine-hydrate, 3,6-di(2-pyridyl)dihydrotetrazine was obtained. Oxidation of this dihydro-tetrazine resulted in the fully-conjugated 3,6-di(2-pyridyl)tetrazine. Furthermore, the authors described the synthesis of unsubstituted, phenyl-substituted and cyano-substituted 3,6-di(2-pyridyl)pyridazines by inverse-type Diels−Alder reactions with the corresponding acetylenes. Other groups later reported similar cycloadditions to the 3,6-di(2-pyridyl)tetrazine, resulting in monosubstituted octyl,[8] carboxyethyl,[8] (tetrahydropyranyl) diethyl ethers of methanol,[18] hexanol,[19] and fullerene[20] 3,6-di(2-pyridyl)-pyridazines. Furthermore, cyclic aliphatic 3,6-di(2-pyridyl)-pyridazines have also been synthesized. In this class of compounds, cyclooctyne could be coupled most easily to the tetrazine, because of the large relief of ring strain in the reaction.[21] Other cyclic substituted 3,6-di(2-pyridyl)pyridazines were synthesized by Diels−Alder reactions with 1-morpholinocycloalkenes, followed by oxidative elimination with hydrogen peroxide.[22] In this case, the electron-donating morpholino group accelerated the inverse electron demand Diels−Alder reaction.[23]

In this study, we chose to investigate, in particular, the Diels−Alder reaction of alkynes with 3,6-di(2-pyridyl)-1,2,4,5-tetrazine, since this results directly in the desired 3,6-di(2-pyridyl)pyridazines as depicted in Scheme 1. Moreover, for the preparation of a wide range of different 3,6-di(2-pyridyl)pyridazines, it is not necessary to use alkenes in the synthetic route, since many alkynes are commercially available nowadays.

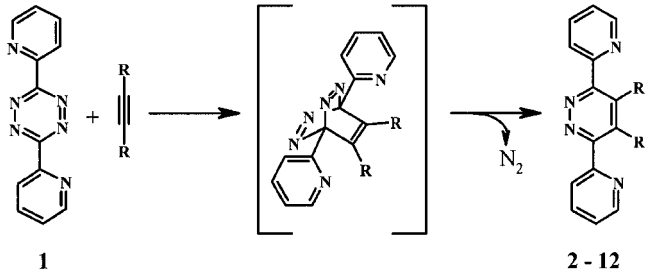

Scheme 1. Schematic representation of the investigated inverse electron demand Diels−Alder reaction between 3,6-di(2-pyridyl)-1,2,4,5-tetrazine and acetylenes

Cycloadditions of alkynes to 3,6-di(2-pyridyl)-1,2,4,5-tetrazine are generally slow reactions; whereby the disappearance of the intense violet color of the tetrazine indicates the progress of the reaction. The reaction conditions, purification methods and yields for the syntheses of the novel 4,5-substituted 3,6-di(2-pyridyl)pyridazines are shown in Table 1. Reactions with hydroxy-functionalized acetylenes were all performed in refluxing toluene. Column chromatography of the crude products resulted in both an orange fraction (identified as 3,6-di(2-pyridyl)-1,4-dihydro-1,2,4,5-tetrazine) and a fraction containing the expected compounds **3**−**8**. Until now, the direct hetero-Diels−Alder reaction between a hydroxy-functionalized alkyne and a tetrazine has not been reported. For the cycloaddition of aliphatic acetylenes to 3,6-di(2-pyridyl)-1,2,4,5-tetrazine, more stringent reaction conditions (refluxing DMF) were required, because the absence of electron-rich groups results in lower reactivity. Even 10-undecyn-1-ol, where the hydroxyl group is far away from the triple bond, is more reactive in the inverse electron demand Diels−Alder reaction than, for example, 1-undecyne. This might be due to the comparable polarity of the hydroxyl group and the pyridines, which could lead to the closer proximity of the reactants, and thus a faster reaction. Cycloaddition of the even less reactive 3-hexyne to the tetrazine was also attempted in refluxing DMF. After several days, a dark brown reaction mixture was obtained, from which a very small fraction of product could be isolated. However, this fraction was not pure and the amount was too small for further purification steps to be carried out. In addition, more electron-rich alkynes (propargyl chloride, 1,4-dichloro-2-butyne, acetylenedicarboxylic acid and tributylstannylacetylene) were also tested in the inverse electron demand Diels−Alder reaction. The reaction mixtures with the chloro- and acid-substituted acetylenes turned black, whereas the bulky tributylstannyl-acetylene reacted successfully with 3,6-di(2-pyridyl)-1,2,4,5-tetrazine, resulting in 3,6-di(2-pyridyl)-4-(tributylstannyl)pyridazine (**12**). Other bulky acetylenes, such as 2-butyn-1,4-diol diacetate and *tert*-butylacetylene, could not be coupled to the tetrazine, which indicates that the electron-rich tributylstannyl group may have a large influence on the outcome of the reaction.

X-ray Crystal Structures of Substituted 3,6-Di(2-pyridyl)-pyridazines

Single crystals suitable for X-ray analysis were obtained for 4,5-bis(hydroxymethyl)-3,6-di(2-pyridyl)pyridazine (**8**), 4-butyl-3,6-di(2-pyridyl)pyridazine (**9**), and 3,6-di(2-pyridyl)-4-(tributylstannyl)pyridazine (**12**) as described in the Exp. Sect. The observed molecular structures (ORTEP plot) and the packing diagrams of these compounds are shown in Figure 2. Selected bond lengths and angles for **8**, **9**, and **12** are given in Tables 2, 3, and 4, respectively.

The most intriguing difference between the bis(hydroxymethyl)-substituted pyridazine and the other two compounds is the torsion angle between the inner and the outer rings, which is 43.5° between the mean plane through the central aromatic ring N(1)−C(6) and the outer pyridine ring C(7)−C(12), and 40.5° between the central ring and C(13)−C(18). The resulting torsion between the mean planes of the outer rings [C(7)−C(12)/C(13)−C(18)] is 13.7°. In compound **9**, the torsion angles are much smaller: N(1)−C(12)/C(7)−C(12): 9.3°, N(1)−C(12)/C(13)−C(18): 12.9°, and C(7)−C(12)/C(13)−C(18): 22.1°. This difference is most likely due to the formation of hydrogen bonds between the nitrogen atoms of the pyridyl rings and the hydroxyl groups of the substituents, whereby seven-membered rings are formed. This is supported by the rather short nitrogen−oxygen distances which are in the range of hydrogen bonds [N(8)−O(20): 276.9 pm; N(14)−O(22): 274.1

Table 1. Reactions conditions for the synthesis of the different 3,6-di(2-pyridyl)pyridazines from 3,6-di(2-pyridyl)-1,2,4,5-tetrazine with varying acetylenes. Preparative chromatography of all compounds was performed on aluminum oxide columns

Compound	Dienophile	Solvent (reflux)	Reaction time	Column eluent	Recrystallized from	Yield (%)
2[a]	NEt_2	CCl_4	1 h	$CHCl_3$	EtOH	80
3	$HC{\equiv}CCH_2OH$	toluene	75 h	EA	Et_2O:CH_2Cl_2	88
4	$HC{\equiv}C(CH_2)_2OH$	toluene	75 h	EA	Et_2O (−25 °C)	77
5	$HC{\equiv}C(CH_2)_3OH$	toluene	40 h	$CHCl_3$	$CHCl_3$:Et_2O:*n*-hexane	80
6	$HC{\equiv}C(CH_2)_4OH$	toluene	40 h	$CHCl_3$	$CHCl_3$:Et_2O:*n*-hexane	70
7	$HC{\equiv}C(CH_2)_9OH$	toluene	75 h	$CHCl_3$	Et_2O (−25 °C)	89
8	$HOCH_2C{\equiv}CCH_2OH$	toluene	40 h	$CHCl_3$	EtOH	71
9	$HC{\equiv}C(CH_2)_3CH_3$	DMF	16 h	$CHCl_3$	EtOH/H_2O	71
10[b]	$HC{\equiv}C(CH_2)_8CH_3$	DMF	16 h	−	MeOH/H_2O	58
11	$HC{\equiv}C(CH_2)_{13}CH_3$	DMF	16 h	−	MeOH/H_2O	57
12	$HC{\equiv}CSn(But)_3$	toluene	75 h	$CHCl_3$	−	70
	$CH_3CH_2C{\equiv}CCH_2CH_3$	DMF	120 h	*no pure product could be isolated*		
	$HC{\equiv}CCH_2Cl$	toluene	10 h	*decomposition of reactants*		
	$ClCH_2C{\equiv}CCH_2Cl$	toluene	10 h	*decomposition of reactants*		
	HOOCC≡CCOOH	toluene	10 h	*decomposition of reactants*		

[a] Conditions were similar to those reported in literature procedures (see ref.[30]). [b] Conditions were similar to those reported in literature procedures (see ref.[8]).

pm].[24] The hydrogen bonds are probably also the reason that the outer rings are not collinear but bend away from the substituents resulting in different angles of the connecting bonds [N(2)−C(3)−C(7): 112.98(15); C(4)−C(3)−C(7): 123.52(16); N(1)−C(6)−C(13): 113.10(15); C(5)−C(6)−C(13): 123.71(16)]. This distortion is nearly symmetrical in compound **8**. A similar distortion can also be observed in compound **9**, however, there it is unsymmetrical and is particularly pronounced for the pyridine moiety adjacent to the substituent. Therefore, it can be led back to a steric effect of the substituent [N(1)−C(6)−C(13): 112.28(14); C(5)−C(6)−C(13): 126.03(14); N(2)−C(3)−C(7): 116.71(13); C(4)−C(3)−C(7): 123.52(16)].

The molecular structure of compound **12** is somewhat different to the other two molecules. The torsion of the aromatic rings against each other is smaller C(7)−C(12)/N(1)−C(6): 7.2°, C(7)−C(12)/C(13)−C(18): 10.3°, N(1)−C(6)/C(13)−C(18): 17.3°. This can be partially explained by an intramolecular nitrogen-tin interaction leading to a weak pentacoordination of the tin atom. This is seen in the short Sn−N distance [Sn(1)−N(1): 277.1 pm], and supported by the deviation from tetrahedral of the coordination-geometry around the tin atom [mean angle C(12)−Sn(1)−C(23), C(19)−Sn(1)−C(23), C(23)−Sn(1)−C(27): 103.4° vs. C(12)−Sn(1)−C(19), C(12)−Sn(1)−C(27), C(19)−Sn(1)−C(27): 114.75]. Therefore, the tin atom can be described to be in a pseudo-trigonal bipyramidal coordination-sphere, which is known for several molecules with intramolecular Sn−N interactions.[25,26] Typically, such a distortion around the tin atom is accompanied by a lengthening of the Sn−C bond in the *trans*-position to the Sn−N interaction, if similar substituents are present at the Sn atom. This effect can also be observed in compound **12** if the three $Sn-C_{alkyl}$ bond lengths are compared: an increase of the bond length of 3 pm is detected [Sn(1)−C(12): 217.6(3) vs. Sn(1)−C(19): 214.6(3), Sn(1)−C(27): 214.7(3)].

For all compounds, extensive π−π stacking in the packing diagrams between the aromatic systems can be observed (Figure 2).

Nuclear Magnetic Resonance (NMR) Spectroscopic Investigations

In view of the importance of the class of ligands under investigation, and in order to allow a comparison with the corresponding metal complexes, the 3,6-di(2-pyridyl)pyridazines **2**−**12** obtained were characterized in detail with ^1H NMR and ^{13}C NMR spectroscopy, ^1H-^1H correlated spectroscopy (COSY) and ^1H-^{13}C heteronuclear multiple quantum coherence (HMQC) (all in deuterated chloroform).[27] By combining these NMR techniques, almost all the chemical shifts of the protons and carbon atoms could be assigned, in particular, in the cases where different resonances were observed for the protons and carbon atoms of the two pyridine rings from the monofunctionalized compounds. However, the chemical shifts of the CH4 and CH4′′ protons and also those of the CH5 and CH5′′ protons appear at the same chemical shift for compounds **6**, **7**, **9**−**11**, whereas the carbon signals are different. Therefore, an assignment of the carbon atoms was not possible using HMQC spectroscopy. In order to solve this problem, an incredible natural abundance double-quantum transfer experiment (2D ^{13}C-^{13}C INADEQUATE) was performed on 4-octyl-2,6-di(2-pyridyl)pyridazine **10**. The detection of coupled ^{13}C resonances is very difficult, and requires a signal to noise ratio larger than 20 for a one-transient ^{13}C spectrum. This was achieved by dissolving ca. 500 mg of compound **10** in 1 mL of $CDCl_3$. Figure 3 (left) depicts the 2D INADEQUATE spectrum we obtained, in which all dipolar coupled two-spin systems result in horizontally-connected ^{13}C-^{13}C doublets that cross the skew diagonal of slope 2. These horizontal slices are located at the sum of the resonances of the two coupled carbon atoms on the vertical scale. From this experiment, all the carbon resonances could be unam-

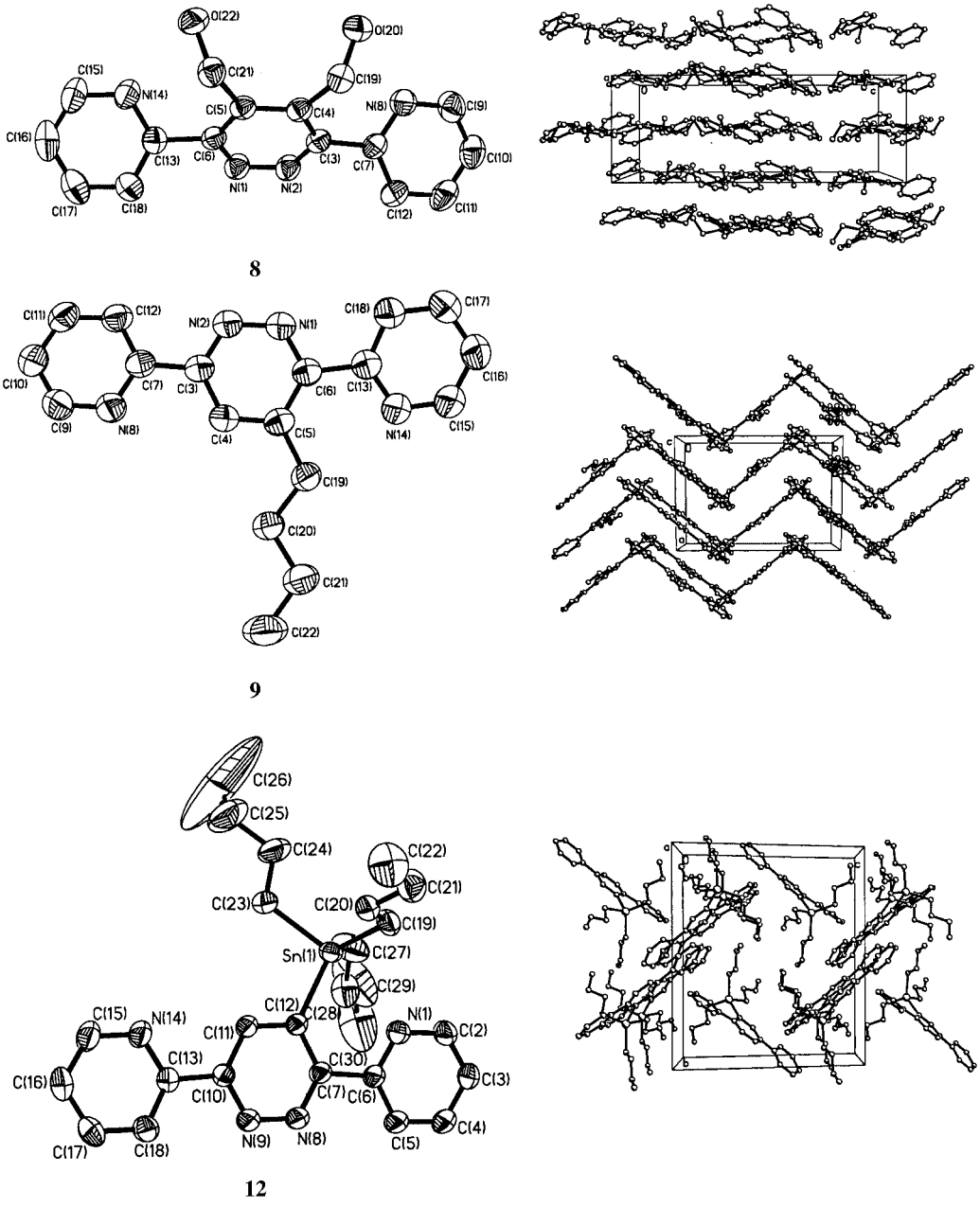

Figure 2. ORTEP plots (50% probability) and packing diagrams of the structures of 4,5-bis(hydroxymethyl)-3,6-di(2-pyridyl)pyridazine (**8**) (top), 4-butyl-3,6-di(2-pyridyl)pyridazine (**9**) (middle), and 3,6-di(2-pyridyl)-4-(tributylstannyl)pyridazine (**12**) (bottom). Hydrogen atoms are omitted for clarity

biguously assigned for 4-octyl-2,6-di(2-pyridyl)pyridazine (**10**), and thus also for compounds **6**, **7**, **9**, and **11**.

For the hydroxyl-functionalized compounds **2**−**8**, the chemical shifts of the hydroxyl groups appear as sharp triplets; at 2.01 ppm for the compounds with butyl (**6**) and nonyl (**7**) spacers, at 5.36 ppm for the hydroxypropyl-substituted compound **5**, and higher than 6 ppm for the other three compounds with shorter spacers (**3**, **4**, and **8**). This suggests that intramolecular hydrogen bonding is present in chloroform solution for the compounds with hydroxymethyl (**3**, **8**) and hydroxyethyl (**4**) substituents. This was proved for 4,5-bis(hydroxymethyl)-3,6-di(2-pyridyl)pyridazine (**8**) by nuclear Overhauser effect spectroscopy (NOESY) that demonstrated the through-space coupling of the hydroxyl protons with the H-6 protons (Figure 3, right).

Solid-state ATR-FTIR of the hydroxymethyl functionalized compounds **3** and **8** also demonstrated intramolecular hydrogen bonding between the OH and the nitrogen atoms of the outer pyridyl rings (hydroxyl stretch vibration at 3200 cm^{-1}) as was also seen in the X-ray structure of **8**. The hydroxyethyl-substituted dipyridyl-pyridazine **4** shows two hydroxyl vibrations at 3200 and 3350 cm^{-1}, which suggests that both intramolecular and intermolecular hydrogen bonding occurs. For the other hydroxy-functionalized com-

Table 2. Selected bond lengths [pm] and angles [°] for **8**

N(1)−N(2)	133.7(2)	N(1)−N(2)−C(3)	119.55(15)
N(1)−C(6)	133.7(2)	N(2)−C(3)−C(4)	123.50(16)
N(2)−C(3)	133.4(2)	N(2)−C(3)−C(7)	112.98(15)
C(4)−C(19)	151.2(2)	C(4)−C(3)−C(7)	123.52(16)
C(5)−C(21)	151.1(2)	C(3)−C(4)−C(19)	119.84(15)
C(7)−N(8)	133.6(2)	C(6)−C(5)−C(21)	120.06(15)
N(8)−C(9)	133.8(2)	N(1)−C(6)−C(5)	123.18(16)
C(13)−N(14)	134.0(2)	N(1)−C(6)−C(13)	113.10(15)
N(14)−C(15)	133.3(3)	C(5)−C(6)−C(13)	123.71(16)
C(19)−O(20)	141.7(2)	C(7)−N(8)−C(9)	117.59(17)
C(21)−O(22)	142.1(2)	C(15)−N(14)−C(13)	117.71(18)
		O(20)−C(19)−C(4)	111.88(15)
N(2)−N(1)−C(6)	119.84(15)	O(22)−C(21)−C(5)	111.14(15)

Table 3. Selected bond lengths [pm] and angles [°] for **9**

N(1)−N(2)	133.48(19)	N(1)−N(2)−C(3)	119.32(13)
N(1)−C(6)	134.0(2)	N(1)−C(6)−C(13)	112.28(14)
N(2)−C(3)	133.0(2)	C(5)−C(6)−C(13)	126.03(14)
C(5)−C(19)	151.0(2)	N(2)−C(3)−C(4)	121.58(15)
C(7)−N(8)	133.6(2)	N(2)−C(3)−C(7)	116.71(13)
N(8)−C(9)	133.5(2)	C(4)−C(3)−C(7)	121.70(14)
C(13)−N(14)	133.0(2)	C(4)−C(5)−C(19)	120.14(14)
N(14)−C(15)	133.8(3)	C(9)−N(8)−C(7)	117.37(15)
		C(13)−N(14)−C(15)	117.36(17)
N(2)−N(1)−C(6)	121.55(13)		

Table 4. Selected bond lengths [pm] and angles [°] for **12**

Sn(1)−C(12)	217.3(2)	C(12)−Sn(1)−C(19)	113.13(10)
Sn(1)−C(19)	214.6(3)	C(12)−Sn(1)−C(23)	99.65(10)
Sn(1)−C(23)	217.6(3)	C(12)−Sn(1)−C(27)	116.05(12)
Sn(1)−C(27)	214.7(3)	C(19)−Sn(1)−C(23)	104.89(11)
N(1)−C(2)	134.1(3)	C(19)−Sn(1)−C(27)	115.07(14)
N(1)−C(6)	133.0(3)	C(23)−Sn(1)−C(27)	105.77(16)
C(7)−N(8)	133.5(3)	C(2)−N(1)−C(6)	118.6(2)
N(8)−N(9)	133.9(3)	C(7)−N(8)−N(9)	120.1(2)
N(9)−C(10)	133.7(3)	C(10)−N(9)−N(8)	119.1(2)
C(13)−N(14)	133.8(3)	C(11)−C(12)−Sn(1)	120.50(17)
N(14)−C(15)	133.6(3)	C(7)−C(12)−Sn(1)	124.96(16)
		C(13)−N(14)−C(15)	117.1(2)

pounds **5**−**7**, the hydroxyl stretch vibrations are between 3300 and 3500 cm^{-1}, indicating intermolecular hydrogen bonding in the solid state.

Complexation Studies of Functionalized 3,6-Di(2-pyridyl)-pyridazines

The potential for supramolecular self-assembly of the functionalized 3,6-di(2-pyridyl)pyridazines into grid-like complexes with copper(I) and silver(I) ions (see Figure 1) was investigated using 4,5-bis(hydroxymethyl)-3,6-di(2-pyridyl)pyridazine (**8**) as a ligand. This ligand was chosen because of its rigid conformation arising from intramolecular hydrogen bonding. Thus, if this ligand would self-assemble into grid-like complexes and thus act as a coordinating ligand for copper(I) and silver(I) ions (with the loss of the hydrogen-bonding interactions), similar behavior could be expected for the other functionalized dipyridylpyridazines.

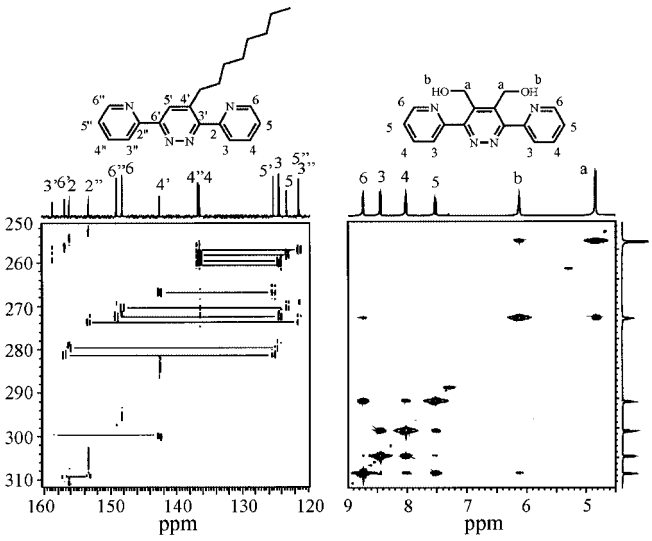

Figure 3. ^{13}C-^{13}C INADEQUATE measured from 4-octyl-3,6-di(2-pyridyl)pyridazine (**10**) (left); NOESY spectrum of 4,5-bis(hydroxymethyl)-3,6-di(2-pyridyl)pyridazine (**8**) (right, both spectra were recorded in $CDCl_3$)

Self-assembly of the grids with copper(I) ions was performed by adding a solution of the 4,5-bis(hydroxymethyl)-3,6-di(2-pyridyl)pyridazine ligand (**8**) (1 equiv.) in dichloromethane to a solution of tetrakis(acetonitrile)copper(I) hexafluorophosphate (1 equiv.) in dichloromethane, resulting in the instantaneous formation of copper-grid **13** as a brown precipitate. The silver(I)-grid **14** was prepared in a similar way, whereby the ligand **8** (1 equiv.) in dichloromethane was added to a solution of silver(I)tetrafluoroborate (1 equiv.) in a dichloromethane/acetonitrile mixture (10:1), resulting in the immediate precipitation of the product as a white solid. The copper-grid **13** appeared to be soluble only in acetone and methanol, whereas the silver-grid **14** was soluble only in nitromethane (the free ligands and the metal salts are both highly soluble in dichloromethane). Previously reported [2 × 2] and similar larger silver(I)-grids are also known to dissolve only in nitromethane.[3,28,29] ^1H NMR spectroscopic investigations revealed only four aromatic signals for the obtained grids **13** and **14** (Figure 4). This demonstrates the high symmetry of the complexes, and thus suggests the formation of defined grid-like architectures rather than polymeric species. All the signals in the spectra of the grids appear broader than the signals in the spectra of the pure ligand, and the 3-H and 6-H protons switch positions upon complexation with both copper(I) and silver(I) ions. This is also a proof for the successful complexation. IR spectroscopic investigations revealed a significant difference in the C=N and OH stretch vibrations upon complexation with both copper(I) and silver(I) ions. Grid-formation with copper(I) ions resulted in the appearance of a C=N vibration at 1594 cm^{-1}, whereas ligand **8** has two signals at 1590 and 1569 cm^{-1}. A similar shift in C=N stretch vibrations was also reported for the formation of copper(I)-grids from the unfunctionalized 3,6-di(2-pyridyl)pyridazine.[2] In case of the silver(I)-grid, the

C=N stretch vibrations appear at 1597 and 1571 cm^{-1}. The hydrogen-bonded OH stretch vibrations at 3201 cm^{-1} of the free ligand shifted to 3344 and 3481 cm^{-1} for the grid-complexes with copper(I) and silver(I), respectively, which clearly demonstrates the disappearance of the hydrogen bonding. In addition, the vibrations of the PF_6 and BF_4 counterions appear as strong bands at 833 cm^{-1} for the copper-complex **13** and around 1030 cm^{-1} for the silver-complex **14**. Figure 5 depicts the UV/Vis spectra of both ligand **8** and copper-grid **13**. Silver-grid **14** could not be characterized with UV/Vis spectroscopy, since it is only soluble in nitromethane, and this solvent absorbs strongly at wavelengths shorter than 350 nm. Figure 5 clearly shows the appearance of a second absorption maximum at 436 nm upon complexation with copper(I) ions. Such an observation has also been described in the literature in the formation of copper-grids with the unsubstituted 3,6-di(2-pyridyl)-pyridazine **2**.[2] ESI-QTOF-MS of **13** revealed the existence of complete [2×2] copper(I) grids as shown in the inset of Figure 5. The inset depicts a single charged grid with three counterions. The isotopic pattern matches exactly with a simulated spectrum. Doubly- and triply-charged grids were also observed (not shown). Furthermore, complexes with two or three ligands containing one, two or three copper(I) ions resulting from fragmentation of the grids were also observed in the spectrum. The high symmetry of the complexes formed, as revealed by NMR spectroscopy together with the additional characterization utilizing IR and UV/Vis spectroscopy and ESI-QTOF-MS, clearly show that even though the structure of 4,5-bis(hydroxymethyl)-3,6-di(2-pyridyl)pyridazine (**8**) is stabilized by intramolecular hydrogen bonding, the compound is still capable of flipping the outer rings to act as a ligand for copper(I) and silver(I) ions, thus forming grid-like architectures. Therefore, it will also be possible to form similar grid-like complexes with the other functionalized 3,6-di(2-pyridyl)pyridazines as was also recently demonstrated for 4-(1-hydroxybutyl)-3,6-di(2-pyridyl)pyridazine (**6**) and similar polymeric ligands with copper(I) ions.[9]

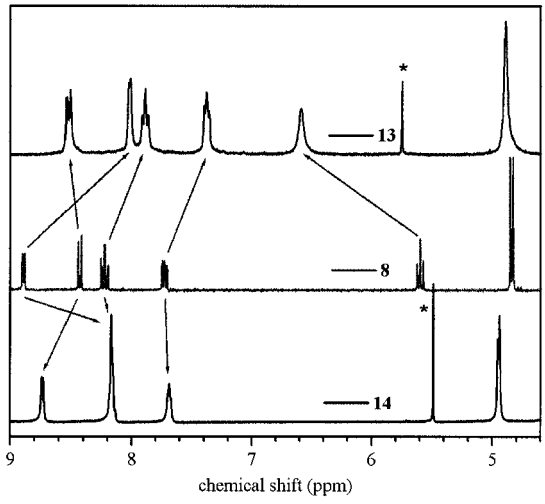

Figure 4 .^{1}H NMR spectra of ligand **8** (middle, [D_6]acetone) and the corresponding copper (top, [D_6]acetone) and silver (bottom, CD_3NO_2) grids

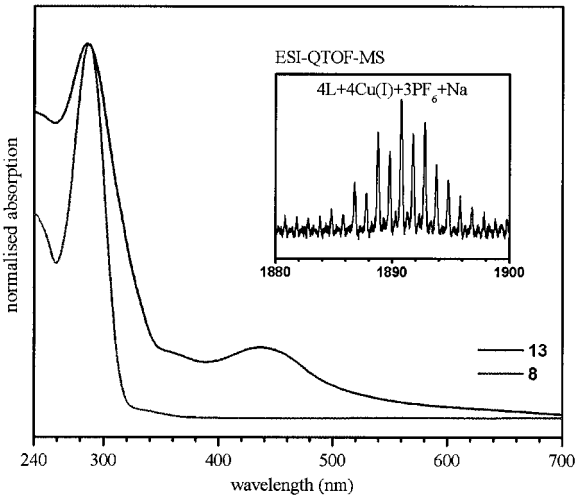

Figure 5. UV/Vis spectra of 4,5-bis(hydroxymethyl)-3,6-di(2-pyridyl)pyridazine (**8**) (chloroform) and the corresponding copper grid **13** (methanol). The inset shows an enlargement of the ESI-QTOF-MS spectrum proving the existence of complete [2×2] grids

Conclusion

Inverse electron demand Diels−Alder reactions between 3,6-di(2-pyridyl)-1,2,4,5-tetrazine (**1**) and various (functional) alkynes have been described.

X-ray crystal structures were obtained for 4,5-bis(hydroxymethyl)-3,6-di(2-pyridyl)pyridazine (**8**), 4-butyl-3,6-di(2-pyridyl)pyridazine (**9**), and 3,6-di(2-pyridyl)-4-(tributylstannyl)pyridazine (**12**), whereby the structure of **8** clearly revealed the presence of intramolecular hydrogen bonding between the hydroxyl groups and the nitrogen atoms of the outer pyridyl rings, and the structure of **12** revealed an intramolecular nitrogen-tin interaction leading to a weak pentacoordination of the tin atom. In all compounds, extensive π−π stacking in the packing diagrams between the aromatic systems was observed (Figure 2).

For a complete assignment of all proton and carbon resonances, ^{1}H-^{1}H COSY, ^{1}H-^{13}C HMQC, and ^{13}C-^{13}C INADEQUATE measurements were performed. Moreover, a NOESY experiment demonstrated the through-space coupling of the hydroxyl protons of 4,5-bis(hydroxymethyl)-3,6-di(2-pyridyl)pyridazine (**8**) with the 6-H protons, thus proving that intramolecular hydrogen bonding exists in chloroform solution.

The self-assembly of the functionalized 4,5-bis(hydroxymethyl)-3,6-di(2-pyridyl)pyridazine (**8**) with copper(I) and silver(I) ions into [2 × 2] grids was demonstrated by a combination of NMR spectroscopy, IR spectroscopy, and ESI-QTOF-MS.

Further investigations regarding the metal-grids including X-ray crystal structure analysis and scanning tunneling microscopy are ongoing. Moreover, other functional groups will be connected to these 3,6-di(2-pyridyl)pyridazines and

the corresponding grid-like metal complexes via coupling with to hydroxyl group, or via Stille coupling with the tributylstannyl group.

Experimental Section

General Remarks: Solvents were purchased from Biosolve and all other compounds were obtained from Aldrich or Fluka. All compounds were used without further purification. ^{1}H NMR, ^{1}H-^{1}H COSY, and ^{13}C NMR spectra were recorded on a Varian Mercury 400 spectrometer or a Varian Gemini 300 spectrometer. NOESY, ^{1}H-^{13}C HMQC, and 2D ^{13}C-^{13}C INADEQUATE (delay time = 1.5 s, τ = 4.2 ms) spectra were recorded on a Varian Inova 500 spectrometer; the HMQC experiments were performed with an indirect probe. Chemical shifts are given in ppm relative to TMS or solvent signals for proton and carbon spectra. UV/Vis spectroscopy was done on a Perkin−Elmer Lambda 45 apparatus utilizing 1 cm cuvets. MALDI-TOF-MS was performed on a Voyager-DE™ PRO Biospectrometry™ Workstation (Applied Biosystems) time-of-flight mass spectrometer using linear mode for operation. The spectra were obtained in the positive ion mode, ionization was performed with a 337 nm pulsed nitrogen laser, and dithranol was used as matrix. Data were processed using the Data Explorer™ software package (Applied Biosystems). ESI-QTOF-MS was performed on a Micromass Q-TOF Ultima global apparatus. IR spectra were recorded on a Perkin−Elmer 1600 FT-IR. Elemental analyses were performed on a Carlo Erba Instruments EA1108 CHNS/O Elemental Analyzer and melting points were determined utilizing a Büchi B-540 apparatus.

3,6-Di(2-pyridyl)tetrazine (1): This compound was synthesized as reported in the literature (51.7% overall yield for two reaction steps). M.p. 219−220 °C (ref.[12] 222 °C). ^{1}H NMR ($CDCl_3$): δ 0 8.99 (dd, *J* = 3.9, 1.1 Hz, 2 H, 6,6′′-H), 8.75 (d, *J* = 7.7 Hz, 2 H, 3,3′′-H), 8.01 (dt, *J* = 7.7, 1.6 Hz, 2 H, 4,4′′-H), 7.58 (dt, *J* = 3.9, 1.1 Hz, 1 H, 5,5′′-H) ppm. ^{13}C NMR ($CDCl_3$): δ 0 163.7 (C-3′,6′), 150.9 (C-2,2′′), 150.0 (C-6,6′′), 137.4 (C-4,4′′), 126.5 (C-5,5′′), 124.5 (C-3,3′′) ppm. IR (ATR): $\tilde{\nu}$ = 0 3097 cm^{-1}, 3061, 3047, 1582, 1387, 1259, 1240, 128, 993, 919, 796, 743, 732, 594. MALDI-TOF-MS: *m*/*z* = [M$^+$] 237 (100%). UV/Vis (chloroform): λ_{max} = 546 nm, 293 nm.

3,6-Di(2-pyridyl)pyridazine (2): 3,6-Di(2-pyridyl)pyridazine (**2**) was synthesized as described in the literature (81% yield). M.p. 178−179 °C (ref.[25] 179−180 °C). ^{1}H NMR ($CDCl_3$): δ = 8.80 (m, 4 H, 6,6′′,3,3′′-H), 8.75 (s, 2 H, 4′,5′-H), 7.97 (dt, *J* = 7.7, 2.2 Hz, 2 H, 4,4′′-H), 7.47 (dt, *J* = 7.7, 1.1 Hz, 1 H, 5,5′′-H) ppm. ^{13}C NMR ($CDCl_3$): δ = 158.0 (C-3′,6′), 153.2 (C-2,2′′), 150.0 (C-6,6′′), 137.2 (C-4,4′′), 125.1 (C-4′,5′), 124.7 (C-5,5′′), 121.6 (C-3,3′′) ppm. IR (ATR): $\tilde{\nu}$ = 3053 cm^{-1}, 1585, 1570, 1414, 988, 872, 778, 747, 726. MALDI-TOF-MS: *m*/*z* = [M$^+$] 235 (100%). UV/Vis (chloroform): λ_{max} = 299 nm.

4-(Hydroxymethyl)-3,6-di(2-pyridyl)pyridazine (3): A solution of 3,6-di(2-pyridyl)tetrazine (**1**, 500 mg, 2.12 mmol) and propargyl alcohol (238 mg, 4.24 mmol) in toluene (50 mL) was refluxed for 75 hours. After evaporation of the solvent under reduced pressure, the crude product was purified by column chromatography (Al_2O_3, ethyl acetate as eluent). After recrystallization from diethyl ether/dichloromethane (2:1) at −25 °C, the product was obtained as white needles (480 mg, 88%). M.p. 128−129 °C (decomposition). ^{1}H NMR [$CDCl_3$, ^{1}H-^{1}H correlated spectroscopy (COSY)]: δ = 8.72 (m, 4 H, 3′′,5′,6,6′′-H), 8.53 (d, *J* = 8.1 Hz, 1 H, 3-H), 7.95 (dt, *J* = 8.1, 1.5 Hz, 1 H, 4-H), 7.88 (dt, *J* = 7.3, 2.2 Hz, 1 H, 4′′-H), 7.44 (t, 5.9 Hz, 1 H, 5-H), 7.39 (t, *J* = 3.7 Hz, 1 H, 5′′-H), 6.55 (s, 1 H, O*H*), 4.81 (d, *J* = 5.9 Hz, 2 H, CH_2OH) ppm. ^{13}C NMR [$CDCl_3$, ^{1}H-^{13}C heteronuclear multiple quantum coherence (HMQC)]: δ = 158.0 (C-3′), 157.7 (C-6′), 155.0 (C-2), 152.9 (C-2′′), 149.4 (C-6′′), 148.0 (C-6), 140.2 (C-4′), 137.7 (C-4), 137.0 (C-4′′), 125.4 (C-5′), 124.8 (C-3,5′′), 124.3 (C-5), 121.5 (C-3′′), 63.0 (*C*H$_2$OH) ppm. IR (ATR): $\tilde{\nu}$ = 3296 cm^{-1}, 3092, 3063, 1585, 1568, 1399, 1050, 992, 786, 737, 619. $C_{15}H_{12}N_4O$: calcd. C 68.17, H 4.58, N 21.20; found C 68.01, H 4.50, N 20.90. MALDI-TOF-MS: *m*/*z* = [M$^+$] 265 (100%). UV/Vis (chloroform): λ_{max} = 295 nm.

4-(1-Hydroxyethyl)-3,6-di(2-pyridyl)pyridazine (4): A solution of 3,6-di(2-pyridyl)tetrazine (**1**, 500 mg, 2.12 mmol) and 3-butyn-1-ol (300 mg, 4.24 mmol) in toluene (50 mL) was refluxed for 75 hours. After evaporation of the solvent under reduced pressure, the crude product was purified by column chromatography [Al_2O_3, gradient from ethyl acetate to ethanol/ethyl acetate (1:9) as eluent]. Recrystallization from diethyl ether at −25 °C yielded the product as yellow crystals (456 mg, 77%). M.p. 65−66 °C. ^{1}H NMR ($CDCl_3$, ^{1}H-^{1}H COSY): δ = 8.76 (m, 2 H, 3′′,6′′-H), 8.68 (dd, *J* = 4.4, 1.7 Hz, 1 H, 6-H), 8.62 (s, 1 H, 5′-H), 8.32 (dd, *J* = 8.2, 1.1 Hz, 1 H, 3-H), 8.00 (dt, *J* = 7.7, 1.7 Hz, 1 H, 4-H), 7.91 (dt, *J* = 7.7, 1.7 Hz, 1 H, 4′′-H), 7.49 (dt, *J* = 7.7 Hz, 1.7, 1 H, 5-H), 7.42 (dt, *J* = 7.7 Hz, 1.7, 1 H, 5′′-H), 6.71 (t, *J* = 4.4 Hz, 1 H, O*H*), 4.17 (q, *J* = 5.5, 4.4 Hz, 2 H, CH_2OH), 3.17 (t, *J* = 5.5 Hz, 2 H, CH_2CH$_2$OH) ppm. ^{13}C NMR ($CDCl_3$, ^{1}H-^{13}C HMQC): δ = 158.9 (C-3′), 157.5 (C-6′), 154.8 (C-2), 153.2 (C-2′′), 149.4 (C-6′′), 147.5 (C-6), 140.5 (C-4′), 138.0 (C-4), 137.2 (C-4′′), 126.6 (C-5′), 125.6 (C-3), 124.8 (C-5′′), 124.1 (C-5), 121.8 (C-3′′), 63.3 (*C*H$_2$OH), 34.6 (*C*H$_2$CH$_2$OH) ppm. IR (ATR): $\tilde{\nu}$ = 3353 cm^{-1}, 3158, 3054, 2852, 1579, 1570, 1397, 1074, 1052, 993, 790, 745, 728, 656. $C_{16}H_{14}N_4O$: calcd. C 69.05, H 5.07, N 20.13; found C 68.74, H 4.93, N 19.69. MALDI-TOF-MS: *m*/*z* = [M$^+$] 279 (100%). UV/Vis (chloroform): λ_{max} = 290 nm.

4-(1-Hydroxypropyl)-3,6-di(2-pyridyl)pyridazine (5): A solution of 3,6-di(2-pyridyl)tetrazine (**1**, 500 mg, 2.1 mmol) and 4-pentyn-1-ol (335 mg, 4.2 mmol) in toluene (25 mL) was refluxed for 40 hours. After evaporation of the solvent under reduced pressure, the crude product was purified by column chromatography (Al_2O_3, chloroform as eluent). After recrystallization from chlorofom/diethyl ether/hexane (1:2:1), the product was obtained as yellowish crystals (257 mg, 80%). M.p. 74−76 °C. ^{1}H NMR ($CDCl_3$, ^{1}H-^{1}H COSY): δ = 8.75 (m, 2 H, 3′′,6′′-H), 8.68 (d, *J* = 4.4 Hz, 1 H, 6-H), 8.57 (s, 1 H, 5′-H), 8.19 (d, *J* = 7.3 Hz, 1 H, 3-H), 7.97 (t, *J* = 7.3 Hz, 1 H, 4-H), 7.91 (t, *J* = 7.3 Hz, 1 H, 4′′-H), 7.46 (t, *J* = 7.3 Hz, 1 H, 5-H), 7.42 (t, *J* = 7.3 Hz, 1 H, 5′′-H), 5.36 (t, *J* = 5.1 Hz, 1 H, O*H*), 3.60 (q, *J* = 5.1 Hz, 2 H, CH_2OH), 3.13 (t, *J* = 7.3 Hz, 2 H, CCH_2), 2.15 (m, 2 H, CH_2CH$_2$OH) ppm. ^{13}C NMR ($CDCl_3$): δ = 158.7 (C-3′), 156.9 (C-6′), 155.4 (C-2), 152.9 (C-2′′), 149.1 (C-6′′), 147.7 (C-6), 141.7 (C-4′), 137.2 (C-4′′), 136.9 (C-4), 125.6 (C-5′), 125.1 (C-3), 124.5 (C-5′′), 123.5 (C-5), 121.4 (C-3′′), 60.2 (*C*H$_2$OH), 32.5 (C*C*H$_2$), 27.5 (*C*H$_2$CH$_2$OH) ppm. IR (ATR): $\tilde{\nu}$ = 3330 cm^{-1}, 2933, 2902, 2865, 1583, 1570, 1400, 1056, 993, 790, 743, 726, 658. $C_{17}H_{16}N_4O$: calcd. C 69.85, H 5.52, N 19.16; found C 69.73, H 5.45, N 18.78. MALDI-TOF-MS: *m*/*z* = [M$^+$] 293 (100%). UV/Vis (chloroform): λ_{max} = 288 nm.

4-(1-Hydroxybutyl)-3,6-di(2-pyridyl)pyridazine (6): A solution of 3,6-di(2-pyridyl)tetrazine (**1**, 500 mg, 2.1 mmol) and 5-hexyne-1-ol (410 mg, 4.2 mmol) in toluene (25 mL) was refluxed for 40 hours. After evaporation of the solvent under reduced pressure, the crude product was purified by column chromatography (Al_2O_3, chloroform as eluent). Recrystallization from chloroform/diethyl ether/

hexane (1:2:1) yielded the product as a white solid (448 mg, 70%). M.p. 79.5−80 °C. ^{1}H NMR ($CDCl_3$): δ = 8.79−8.70 (m, 3 H, 6,3′′,6′′-H), 8.48 (s, 1 H, 5′-H), 8.15 (d, *J* = 8.2 Hz, 1 H, 3-H), 7.88 (dt, *J* = 7.7, 2.2 Hz, 2 H, 4,4′′-H), 7.40 (dt, *J* = 8.2, 2.2 Hz, 2 H, 5,5′′-H), 3.62 (q, *J* = 4.9 Hz, 2 H, CH_2OH), 3.08 (t, *J* = 8.2 Hz, 2 H, CCH_2), 2.01 (t, *J* = 4.9 Hz, 1 H, O*H*), 1.78 (quint, *J* = 8.2 Hz, 2 H, CH_2CH$_2$OH), 1.62 (quint, *J* = 7.2 Hz, 2 H, CCH$_2$CH_2) ppm. ^{13}C NMR ($CDCl_3$): δ = 158.7 (C-3′), 157.0 (C-6′), 155.9 (C-2), 153.1 (C-2′′), 149.1 (C-6′′), 148.3 (C-6), 142.4 (C-4′), 137.0 (C-4′′), 136.8 (C-4), 125.5 (C-5′), 124.7 (C-3), 124.5 (C-5′′), 123.5 (C-5), 121.6 (C-3′′), 61.5 (*C*H$_2$OH), 31.5 (C*C*H$_2$), 31.4 (CCH$_2$*C*H$_2$), 25.8 (*C*H$_2$CH$_2$OH) ppm. IR (ATR): $\tilde{\nu}$ = 3460, 3063, 3017, 2930, 2864, 1580, 1410, 1398, 1054, 1030, 991, 798, 784, 746, 730. $C_{18}H_{18}N_4O$: calcd. C 70.6, H 5.9, N 18.5; found C 71.0, H 5.7, N 18.5. MALDI-TOF-MS: *m*/*z* = [M$^+$] 307 (100%). UV/Vis (chloroform): λ_{max} = 288 nm.

4-(1-Hydroxynonyl)-3,6-di(2-pyridyl)pyridazine (7): A solution of 3,6-di(2-pyridyl)tetrazine (**1**, 500 mg, 2.1 mmol) and 10-undecyn-1-ol (427 mg, 2.5 mmol) in toluene (50 mL) was refluxed for 75 hours. After evaporation of the solvent under reduced pressure, the crude product was purified by column chromatography (Al_2O_3, chloroform as eluent). After recrystallization from diethyl ether, the product was obtained as a white solid (750 mg, 89%). M.p. 71−72 °C. ^{1}H NMR ($CDCl_3$): δ = 8.78−8.74 (m, 3 H, 6,3′′,6′′-H), 8.52(s, 1 H, 5′-H), 8.12 (d, *J* = 8.1 Hz, 1 H, 3-H), 7.92 (t, *J* = 8.1 Hz, 2 H, 4,4′′-H), 7.40 (m, 5,5′′-H), 3.64 (q, *J* = 3.7 Hz, 2 H, CH_2OH), 3.10 (t, *J* = 8.8 Hz, 2 H, CCH_2), 1.62−1.54 (m, 5 H, CCH$_2$CH_2, CH_2CH$_2$OH, and O*H*), 1.30−1.26 (m, 10 H, other CH_2) ppm. ^{13}C NMR ($CDCl_3$): δ = 159.2 (C-3′), 157.3 (C-6′), 156.5 (C-2), 153.7 (C-2′′), 149.4 (C-6′′), 148.6 (C-6), 142.9 (C-4′), 137.2 (C-4′′), 136.9 (C-4), 125.6 (C-5′), 124.8 (C-3), 124.7 (C-5′′), 123.5 (C-5), 121.8 (C-3′′), 63.0 (*C*H$_2$OH), 32.8 (C*C*H$_2$), 32.3 (CCH$_2$*C*H$_2$), 29.7−29.1 (other *C*H$_2$), 25.7 (*C*H$_2$CH$_2$OH) ppm. IR (ATR): $\tilde{\nu}$ = 3328 cm^{-1}, 2926, 3850, 1588, 1579, 1398, 1054, 997, 792, 744, 656, 622, 599. $C_{23}H_{28}N_4O$·???? H_2O: calcd. C 72.51, H 7.54, N 14.70; found C 72.69, H 7.34, N 14.72. MALDI-TOF-MS: *m*/*z* = [M$^+$] 377 (100%). UV/Vis (chloroform): λ_{max} = 286 nm.

4,5-Bis(hydroxymethyl)-3,6-di(2-pyridyl)pyridazine (8): A solution of 3,6-di(2-pyridyl)tetrazine (**1**, 2.0 g, 8.5 mmol) and 2-butyn-1,4-diol (1.5 mg, 17.4 mmol) in toluene (50 mL) was refluxed for 40 hours. The crude reaction mixture was filtered through Al_2O_3 and subsequently the solvent was removed under reduced pressure. Recrystallization from ethanol yielded the product as white needles (1.76 g, 71%). M.p. 198−200 °C (decomposition). ^{1}H NMR ($CDCl_3$, ^{1}H-^{1}H COSY): δ = 8.71 (d, *J* = 5.1 Hz, 2 H, 6,6′′-H), 8.43 (d, *J* = 8.1 Hz, 2 H, 3,3′′-H), 8.00 (dt, *J* = 8.1, 1.5 Hz, 2 H, 4,4′′-H), 7.51 (dt, *J* = 5.1, 1.5 Hz, 2 H, 5,5′′-H), 6.14 (t, *J* = 8.1 Hz, 2 H, O*H*), 4.82 (d, *J* = 8.1 Hz, 4 H, CH_2OH) ppm. ^{13}C NMR ($CDCl_3$, ^{1}H-^{13}C HMQC): δ = 159.2 (C-3′,6′), 155.5 (C-2,2′′), 148.2 (C-6,6′′), 138.2 (C-4′,5′), 138.0 (C-4,4′′), 125.3 (C-3,3′′), 124.5 (C5,5′′), 57.1 (*C*H$_2$OH) ppm. IR (ATR): $\tilde{\nu}$ = 3201 cm^{-1}, 3066, 3005, 2888, 1590, 1569, 1382, 1287, 1214, 1119, 1027, 1013, 1003, 954, 796, 723, 669. $C_{16}H_{14}N_4O_2$: calcd. C 65.30, H 4.79, N 19.04; found C 65.29, H 4.76, N 18.74. MALDI-TOF-MS: *m*/*z* = [M$^+$] 295 (100%). UV/Vis (chloroform): λ_{max} = 289 nm.

4-Butyl-3,6-di(2-pyridyl)pyridazine (9): A solution of 3,6-di(2-pyridyl)tetrazine (**1**, 500 mg, 2.1 mmol) and 1-hexyne (344 mg, 4.2 mmol) in toluene (25 mL) was refluxed for 40 hours. Subsequently, DMF (25 mL) was added, and, after evaporation of the toluene, the reaction mixture was stirred at 160 °C for 16 hours. After evaporation of the solvent under reduced pressure, the crude product was purified by column chromatography (Al_2O_3, chloroform as eluent). After recrystallization from ethanol/water (2:1), the product was obtained as yellowish crystals (434 mg, 71%). M.p. 70−71 °C. ^{1}H NMR ($CDCl_3$, ^{1}H-^{1}H COSY): δ = 8.75−8.70 (m, 3 H, 6,3′′,6′′-H), 8.49 (s, 1 H, 5′-H), 8.09 (d, *J* = 8.1 Hz, 1 H, 3-H), 7.89 (dt, *J* = 8.1, 2.2 Hz, 2 H, 4,4′′-H), 7.40 (dt, *J* = 8.1, 1.5 Hz, 2 H, 5,5′′-H), 3.08 (t, *J* = 8.1 Hz, 2 H, CCH_2), 1.59 (quint, *J* = 7.3 Hz, 2 H, CCH$_2$CH_2), 1.32 (sext, *J* = 7.3 Hz, 2 H, CH_2CH$_3$), 0.86 (t, *J* = 8.1 Hz, 2 H, CH_3) ppm. ^{13}C NMR ($CDCl_3$, ^{1}H-^{13}C HMQC): δ = 159.2 (C-3′), 157.3 (C-6′), 156.5 (C-2), 153.7 (C-2′′), 149.4 (C-6′′), 148.5 (C-6), 142.9 (C-4′), 137.2 (C-4′′), 136.9 (C-4), 125.6 (C-5′), 124.8 (C-3), 124.6 (C-5′′), 123.5 (C-5), 121.8 (C-3′′), 32.0 (C*C*H$_2$), 31.9 (CCH$_2$*C*H$_2$), 22.6 (*C*H$_2$CH$_3$), 13.8 (CH$_2$*C*H$_3$) ppm. IR (ATR): $\tilde{\nu}$ = 3059 cm^{-1}, 2927, 2861, 1579, 1570, 1406, 1378, 1251, 1150, 1099, 991, 801, 780, 744, 728. $C_{18}H_{18}N_4$: calcd. C 74.46, H 6.25, N 19.29; found C 74.44, H 6.09, N 19.04. MALDI-TOF-MS: *m*/*z* = [M$^+$] 291 (100%). UV/Vis (chloroform): λ_{max} = 288 nm.

4-Octyl-3,6-di(2-pyridyl)pyridazine (10): A solution of 3,6-di(2-pyridyl)tetrazine (**1**, 500 mg, 2.1 mmol) and 1-decyne (351 mg, 2.5 mmol) in DMF (50 mL) was refluxed for 16 hours. After evaporation of the solvent under reduced pressure, the crude product was recrystallized from methanol/water (3:1) resulting in a white solid (481 mg, 58%). M.p. 38 °C (ref. 35 °C). ^{1}H NMR ($CDCl_3$): δ = 8.75−8.71 (m, 3 H, 6,3′′,6′′-H), 8.49 (s, 1 H, 5′-H), 8.09 (d, *J* = 8.1 Hz, 1 H, 3-H), 7.89 (dt, *J* = 8.1, 2.2 Hz, 2 H, 4,4′′-H), 7.38 (dt, *J* = 8.1, 1.5 Hz, 2 H, 5,5′′-H), 3.08 (t, *J* = 8.1 Hz, 2 H, CCH_2), 1.60 (quint, *J* = 7.3 Hz, 2 H, CCH$_2$CH_2), 1.31−1.21 (m, 10 H, CH_2), 0.85 (t, *J* = 6.6 Hz, 2 H, CH_3) ppm. ^{13}C NMR [^{13}C-^{13}C incredible natural abundance double-quantum transfer experiment (INADEQUATE), $CDCl_3$]: δ = 159.2 (C-3′), 157.3 (C-6′), 156.5 (C-2), 153.7 (C-2′′), 149.4 (C-6′′), 148.6 (C-6), 142.9 (C-4′), 137.2 (C-4′′), 136.9 (C-4), 125.6 (C-5′), 124.8 (C-3), 124.6 (C-5′′), 123.5 (C-5), 121.8 (C-3′′), 32.3 (C*C*H$_2$), 31.8 (CCH$_2$*C*H$_2$), 29.8 (CCH$_2$CH$_2$*C*H$_2$), 29.5 [C(CH$_2$)$_3$*C*H$_2$], 29.2 [C(CH$_2$)$_4$*C*H$_2$], 29.1 [C(CH$_2$)$_5$*C*H$_2$], 22.7 (*C*H$_2$CH$_3$), 14.1 (CH$_2$*C*H$_3$) ppm. IR (ATR): $\tilde{\nu}$ = 3056 cm^{-1}, 1916, 2851, 1583, 1575, 1469, 1394, 1094, 992, 787, 742, 716, 657, 620, 599. $C_{22}H_{26}N_4$·???? H_2O: calcd. C 75.29, H 7.61, N 15.96; found C 75.63, H 7.22, N 16.17. MALDI-TOF-MS: *m*/*z* = [M$^+$] 347 (100%). UV/Vis (chloroform): λ_{max} = 287 nm.

3,6-Di(2-pyridyl)-4-tridecylpyridazine (11): A solution of 3,6-di(2-pyridyl)tetrazine (**1**, 500 mg, 2.1 mmol) and 1-pentadecyne (530 mg, 2.5 mmol) in DMF (50 mL) was refluxed for 16 hours. After evaporation of the solvent under reduced pressure, the crude product was recrystallized from methanol/water (3:1) resulting in a white solid (536 mg, 57%). M.p. 52−53 °C. ^{1}H NMR ($CDCl_3$): δ = 8.76−8.71 (m, 3 H, 6,3′′,6′′-H), 8.49 (s, 1 H, 5′-H), 8.09 (d, *J* = 7.8 Hz, 1 H, 3-H), 7.89 (dt, *J* = 7.7, 1.6 Hz, 2 H, 4,4′′-H), 7.39 (dt, *J* = 7.7, 1.1 Hz, 2 H, 5,5′′-H), 3.08 (t, *J* = 7.7 Hz, 2 H, CCH_2), 1.60 (quint, *J* = 7.7 Hz, 2 H, CCH$_2$CH_2), 1.29−1.21 (m, 20 H, CH_2), 0.87 (t, *J* = 6.6 Hz, 2 H, CH_3) ppm. ^{13}C NMR ($CDCl_3$): δ = 159.0 (C-3′), 157.1 (C-6′), 156.4 (C-2), 153.6 (C-2′′), 149.2 (C-6′′), 148.4 (C-6), 142.7 (C-4′), 137.0 (C-4′′), 136.7 (C-4), 125.5 (C-5′), 124.9 (C-3), 124.5 (C-5′′), 123.4 (C-5), 121.7 (C-3′′), 32.2 (C*C*H$_2$), 31.8 (CCH$_2$*C*H$_2$), 29.8−29.0 [CCH$_2$CH$_2$(*C*H$_2$)$^{3-11}$], 22.6 (*C*H$_2$CH$_3$), 14.0 (CH$_2$*C*H$_3$) ppm. IR (ATR): $\tilde{\nu}$ = 3054 cm^{-1}, 2964, 2918, 2850, 1583, 1570, 1469, 1421, 1403, 993, 787, 738, 719, 616. $C_{27}H_{36}N_4$: calcd. C 77.84, H 8.71, N 13.45; found C 77.45, H 8.56, N 13.19. MALDI-TOF-MS: *m*/*z* [M$^+$] = 417 (100%). UV/Vis (chloroform): λ_{max} = 287 nm.

3,6-Di(2-pyridyl)-4-(tributylstannyl)pyridazine (12): A solution of 3,6-di(2-pyridyl)tetrazine (**1**, 236 mg, 1.0 mmol) and tributylstannylacetylene (378 mg, 1.2 mmol) in toluene (25 mL) was refluxed for

75 hours. After evaporation of the solvent under reduced pressure, the crude product was purified by column chromatography (Al_2O_3, dichloromethane as eluent). Upon standing the resulting yellow oil crystallized (368 mg, 70%). M.p. 59 °C. ^{1}H NMR ($CDCl_3$, ^{1}H-^{1}H COSY): δ = 8.97 (s, 1 H, 5′-H), 8.94 (d, *J* = 8.1 Hz, 1 H, 3-H), 8.82−8.77 (m, 2 H, 3′′,6-H), 8.64 (d, *J* = 5.2 Hz, 1 H, 6′′-H), 7.96−7.88 (dt, *J* = 8.1, 1.5 Hz, 2 H, H 4,4′′), 7.44−7.38 (dt, *J* = 5.2, 1.5 Hz, 2 H, 5,5′′-H), 1.51 (sext, *J* = 8.1 Hz, 6 H, $SnCH_2CH_2$), 1.32 (sext, *J* = 7.3 Hz, 6 H, CH_2CH_3), 1.16 (t, *J* = 8.1 Hz, 6 H, $SnCH_2$), 0.87 (t, *J* = 7.3 Hz, 9 H, CH_3) ppm. ^{13}C NMR ($CDCl_3$, ^{1}H-^{13}C HMQC): δ = 161.2 (C-3′), 156.0 (C-6′), 154.7 (C-2), 154.2 (C-2′′), 149.5 (C-6), 147.2 (C-6′′), 143.8 (C-4′), 137.5 (C-4), 137.0 (C-4′′), 134.6 (C-5′), 124.5 (C-5′′), 124.3 (C-5), 121.9 (C-3), 121.8 (C-3′′), 29.1 ($SnCH_2$), 27.4 ($SnCH_2CH_2$), 13.7 (CH_2CH_3), 12.8 (CH_2CH_3) ppm. IR (ATR): $\tilde{\nu}$ = 2952 cm^{-1}, 2918, 2868, 2855, 1587, 1571, 1529, 1383, 999, 991, 788, 612. $C_{14}H_{10}N_4$: calcd. C 59.68, H 6.93, N 10.71; found C 59.9, H 6.9, N 10.6. MALDI-TOF-MS: *m*/*z* = [M$^+$] 525 (10%), [M$^+$ − butyl] 467 (90%). UV/Vis (chloroform): λ_{max} = 300 nm, 295 nm.

Copper(I) Grid of 8 (13): A solution of **8** (88.2 mg, 0.30 mmol) in dichloromethane (5 mL) was added dropwise to a solution of tetrakis(acetonitrile)-copper(I)-hexafluorophosphate (112 mg, 0.30 mmol) in dichloromethane (10 mL), which resulted in the instantaneous precipitation of a brown solid. The solid was collected and recrystallized from acetone/diethyl ether (1:1), resulting in complex **13** as a brown solid (135 mg, 90%). ^{1}H NMR ([D$_6$]acetone): δ = 8.52 (d, *J* = 8.2 Hz, 8 H, 3,3′′-H), 8.01 (d, *J* = 3.8 Hz, 8 H, 6,6′′-H), 7.89 (t, *J* = 7.7 Hz, 8 H, 4,4′′-H), 7.38 (t, *J* = 5.5 Hz, 8 H, 5,5′′-H), 6.59 (s, 8 H, O*H*), 5.26 (s, 16 H, CH_2OH). UV/Vis (methanol): λ_{max} = 436 nm, 286 nm. ^{13}C NMR ([D$_6$]acetone): δ = 150.0 (C-6,6′′), 141.1 (C-5,5′′), 128.9 (C-3,3′′), 127.0 (C4,4′′), 57.3 (CH_2OH) ppm. IR (ATR): $\tilde{\nu}$ = 3639 cm^{-1}, 3567, 3344, 3109, 1594, 1465, 1368, 1260, 1033, 1016, 833, 791, 754. ESI-QTOF-MS: *m*/*z* = 1890 ([4L + 4Cu^I + 3PF$_6$ + Na]$^+$), 1153 ([3L + 2Cu^I + 1PF$_6$ + Na]$^+$), 1090 ([2L + 3Cu^I + 2PF$_6$ + Na]$^+$), 887 ([2L + 2Cu^I + PF$_6$]$^+$), 873 ([4L + 4Cu^I + 2PF$_6$ + Na]$^{2+}$), 859 ([2L + Cu^I + PF$_6$]$^+$), 796 ([2L + Cu^I + PF$_6$ + H]$^+$), 651 ([2L + Cu^I]$^+$), 581 ([4L + 4Cu^I + 2PF$_6$ + Na]$^{3+}$) and 532 ([4L + 4Cu^I + PF$_6$ + Na]$^{3+}$).

Silver(I) Grid of 8 (14): A solution of **8** (68 mg, 0.23 mmol) in dichloromethane (5 mL) was added dropwise to a solution of silver(I) tetrafluoroborate (38 mg, 0.20 mmol) in dichloromethane/acetonitrile (5 mL:0.5 mL), which resulted in the instantaneous precipitation of a white solid. After stirring for 15 minutes, the solid was collected and washed several times with dichloromethane, resulting

Table 5. Crystal data and structure refinement

	8	**9**	**12**
Empirical formula	$C_{16}H_{14}N_4O_2$	$C_{18}H_{18}N_4$	$C_{26}H_{36}N_4Sn$
Molecular mass	294.31	290.36	523.28
Temperature [K]	298(2)	294(2)	173(2)
Crystal system	orthorhombic	monoclinic	monoclinic
Space group	*Pbca*	$P2_1/c$	$P2_1/n$
Unit cell dimensions [pm,°]			
a	1674.6(3)	969.1(3)	1013.21(6)
b	781.18(15)	1381.4(4)	1718.17(10)
c	2154.2(4)	1202.3(3)	1519.38(8)
α	90	90	90
β	90	102.313(6)	103.717(1)
γ	90	90	90
Volume [pm^3]	2817.9(9) × 10^6	1572.6(8) × 10^6	2569.6(3) × 10^6
Z	8	4	4
Calculated density [g cm^{-1}]	1.387	1.226	1.353
Absorption coefficient [mm^{-1}]	0.095	0.075	1.013
F(000)	1232	616	1080
Crystal size [mm]	0.40 × 0.08 × 0.06	0.56 × 0.34 × 0.24	0.75 × 0.50 × 0.30
Theta range for data collection [°]	2.25−26.37	2.15−26.37	2.20−28.30
Limiting indices	$-20 \le h \le 20$	$-12 \le h \le 7$	$-13 \le h \le 13$
	$-9 \le k \le 9$	$-17 \le k \le 17$	$-22 \le k \le 22$
	$-23 \le l \le 26$	$-14 \le l \le 15$	$-11 \le l \le 20$
Reflections collected/unique	21827/2878	9429/3212	17833/6369
	[*R*(int) = 0.0546]	[*R*(int) = 0.0306]	[*R*(int) = 0.0572]
Completeness to max.. theta	99.9%	99.9%	99.4%
Max. and min. transmission	0.9943	0.9821	0.7508
	0.9628	0.9590	0.5170
Data/restraints/parameters	2878/0/208	3212/0/272	6369/0/281
Goodness-of-fit on F^2	1.001	1.032	1.035
Final *R* indices [$I > 2\sigma(I)$]	R_1 = 0.0398	R_1 = 0.0462	R_1 = 0.0372
	wR_2 = 0.0892	wR_2 = 0.1208	wR_2 = 0.1044
R indices (all data)	R_1 = 0.0805	R_1 = 0.0716	R_1 = 0.0404
	wR_2 = 0.1089	wR_2 = 0.1381	wR_2 = 0.1082
Extinction coefficient	0.0026(4)	0.0057(17)	0.0004(4)
Largest diff. peak and hole	0.161 and −0.142	0.162 and −0.149	1.086 and −1.019
Weighting scheme[a]	0.0435/0.88	0.0636/0.26	0.0592/1.64
x/*y*			

[a] $W = 1/[\sigma^2(F_o^2) + (x\,P)^2 + y\,P]$, $P = [\max(F_o^2,0) + 2\,F_c^2)/3$.

in compound **14** as a white solid (90 mg, 92%). ^{1}H NMR (CD_3NO_2): δ = 8.70 (d, J = 4.4 Hz, 8 H, 3,3′′-H), 8.13 (m, 16 H, 4,4′′,6,6′′-H), 7.65 (t, J = 4.4 Hz, 8 H, 5,5′′-H), 4.91 (d, J = 5.9 Hz, 16 H, CH_2OH) ppm. ^{13}C NMR (CD_3NO_2): δ = 159.3 (C-3′,6′), 152.1 (C-2,2′′), 150.7 (C-6,6′′), 141.6 (C-4′,5′), 139.4 (C-5,5′′), 126.9 (C-3,3′′), 126.5 (C4,4′′), 57.9 (CH_2OH) ppm. IR (ATR): $\tilde{\nu}$ = 3481 cm^{-1}, 3088, 3068, 1597, 1572, 1477, 1427, 1386, 1065, 1030, 1013, 1004, 792, 785, 757, 722, 670.

X-ray Crystallographic Data: Selected crystals were mounted on a Bruker-AXS APEX diffractometer with a CCD area detector. Graphite-monochromated Mo-K_α radiation (71.073 pm) was used for the measurements. The nominal crystal-to-detector distance was 5.00 cm. A hemisphere of data was collected by a combination of three sets of exposures at 173 K. Each set had a different φ angle for the crystal, and each exposure took 20 s and covered 0.3° in ω. The data were corrected for polarization and Lorentz effects, and an empirical absorption correction (SADABS)[31] was applied. The cell dimensions were refined with all unique reflections. The structures were solved by direct methods (SHELXS-97).[32] Refinement was carried out with the full-matrix least-squares method based on F^2 (SHELXL-97)[32] with anisotropic thermal parameters for all non-hydrogen atoms. Hydrogen atoms were inserted in calculated positions and refined riding with the corresponding atom. Table 5 shows the details of the crystal data and structure refinement.

CCDC-219857 to -219859 contain the supplementary crystallographic data for this paper. These data can be obtained free of charge at www.ccdc.cam.ac.uk/conts/retrieving.html [or from the Cambridge Crystalographic Data Centre, 12 Union Road, Cambridge CB2 1EZ, UK; Fax: (internat.) + 44-1223-336-033; E-mail: deposit@ccdc.cam.ac.uk].

Acknowledgments

The authors would like to thank NWO, the Fonds der Chemischen Industrie, and the Fonds zur Förderung der wissenschaftlichen Forschung (FWF), Austria for financial support of this work. Moreover, we would like to thank Joost van Dongen for the ESI-QTOF-MS, Michael A. R. Meier for the MALDI-TOF-MS, Helene I.V. Amatdjais-Groenen for the elemental analysis, and Marcel van Genderen for his help with the various 2D NMR experiments.

[1] For examples of metal-containing polymers, see: U. S. Schubert, C. Eschbaumer, *Angew. Chem.* **2002**, *114*, 3016−3050; *Angew. Chem. Int. Ed.* **2002**, *41*, 2892−2926.
[2] M.-T. Youinou, N. Rahmouni, J. Fischer, J. A. Osborn, *Angew. Chem.* **1992**, *104*, 771−773; *Angew. Chem. Int. Ed. Engl.* **1992**, *31*, 775−778.
[3] P. N. W. Baxter, J.-M. Lehn, B. O. Kneisel, D. Fenske, *Angew. Chem.* **1997**, *109*, 2067−2070; *Angew. Chem. Int. Ed. Engl.* **1997**, *36*, 1978−1981.
[4] I. Weissbuch, P. N. W. Baxter, I. Kuzmenko, H. Cohen, S. Cohen, K. Kjaer, P. B. Howes, J. Als-Nielsen, J.-M. Lehn, L. Leiserowitz, M. Lahav, *Chem. Eur. J.* **2000**, *6*, 725−734.
[5] N.-D. Sung, K.-S. Yun, T.-Y. Kim, K.-Y. Choi, M. Suh, J.-G. Kim, I.-H. Suh, J. Chin, *Inorg. Chem. Commun.* **2001**, 377−380.
[6] P. W. Ball, A. B. Blake, *J. Chem. Soc., (A)* **1968**, 1415−1422.
[7] G. De Munno, G. Denti, *Inorg. Chim. Acta* **1983**, *74*, 199−203.
[8] M. Ghedini, F. Neve, M. Longeri, M. Bruno, *Inorg. Chim. Acta* **1988**, *149*, 131−138.
[9] R. Hoogenboom, U. S. Schubert, *Macromolecules* **2003**, *36*, 4743−4749.
[10] J. Sauer, *Comprehensive Heterocyclic Chemistry II*, Pergamon: London, **1996**; vol. 6, pp. 901−965.
[11] R. A. Carboni, R. V. Lindsey, *J. Am. Chem. Soc.* **1959**, *81*, 4342−4346.
[12] W. A. Butte, F. H. Case, *J. Org. Chem.* **1961**, *26*, 4690−4692.
[13] D. K. Heldmann, J. Sauer, *Tetrahedron Letters* **1997**, *38*, 5791−5794.
[14] D. L. Boger, R. P. Schaum, R. M. Garbaccio, *J. Org. Chem.* **1998**, *63*, 6329−6337.
[15] T. J. Sparey, T. Harrison, *Tetrahedron Letters* **1998**, *39*, 5873−5874.
[16] J. Sauer, D. K. Heldmann, J. Hetzenegger, J. Krauthan, H. Sichert, J. Schuster, *Eur. J. Org. Chem.* **1998**, 2885−2896.
[17] D. R. Soenen, J. M. Zimpleman, D. L. Boger, *J. Org. Chem.* **2003**, *68*, 3593−3598.
[18] R. A. Russel, D. E. Marsden, M. Sterns, R. N. Warrener, *Aust. J. Chem.* **1981**, *34*, 1223−1234.
[19] EP 293, 078 A1 (**1988**) UPJohn Co. (Invs.: J. M. McCall, D. E. Ayer, E. J. Jacobsen, F. J. VanDoornik, J. R. Palmer).
[20] G. P. Miller, M. C. Tetreau, *Org. Lett.* **2000**, *2*, 3091−3094.
[21] Y. Ikemi, A. Okada, H. Katsura, S. Otani, K. Matsumoto, *Heterocycl. Commun.* **1999**, *5*, 53−38.
[22] M. A. Atfah, *J. Heterocycl. Chem.* **1989**, *26*, 717−719.
[23] J. Sauer, A. Mielert, D. Lang, D. Peter, *Chem. Ber.* **1965**, *98*, 1435−1445.
[24] G. A. Jeffrey (Ed.), *An introduction to hydrogen bonding*, Oxford University Press, Oxford, **1997**.
[25] V. G. K. Das, Lo Kong Mun, C. Wie, S. J. Blunden, T. C. W. Mak, *J. Organomet. Chem.* **1987**, *322*, 163.
[26] J. T. B. H. Jastrzebski, J. Boersma, P. M. Esch, G. van Koten, *Organometallics* **1991**, *10*, 930.
[27] In addition, the reported ^{13}C-resonances for 4′,5′-substituted 3,6-di(2-pyridyl)pyridazines (ref.[8] and A. K. Qisari, *Spectroscopy* **2002**, *16*, 37−41) did not match, which increased our interest in reaching a conclusive assignment.
[28] P. N. W. Baxter, J.-M. Lehn, J. Fischer, M.-T. Youinou, *Angew. Chem.* **1994**, *106*, 2432−2434; *Angew. Chem. Int. Ed. Engl.* **1994**, *33*, 2284−2287.
[29] P. N. W. Baxter, J.-M. Lehn, G. Baum, D. Fenske, *Chem. Eur. J.* **2000**, *6*, 4510−4517.
[30] S. V. Shorsnev, S. E. Esipov, V. V. Kuz'menko, A. V. Gulevskaya, A. F. Pozharskii, A. I. Chernyshev, G. G. Aleksandrov, V. N. Doron'kin, *Khim. Geterotsikl. Soedinenii* **1990**, *11*, 1545−58.
[31] R. H. Blessing, *Acta Crystallogr., Sect. A* **1995**, *51*, 33−38; SADABS: Bruker AXS, **1998**.
[32] G. M. Sheldrick, *SHELX97 Programs for Crystal Structure Analysis* (Release 97−2), University of Göttingen, Göttingen (Germany), **1998**.

Received August 6, 2003

